

ChemComm

Accepted Manuscript



This is an *Accepted Manuscript*, which has been through the Royal Society of Chemistry peer review process and has been accepted for publication.

Accepted Manuscripts are published online shortly after acceptance, before technical editing, formatting and proof reading. Using this free service, authors can make their results available to the community, in citable form, before we publish the edited article. We will replace this *Accepted Manuscript* with the edited and formatted *Advance Article* as soon as it is available.

You can find more information about *Accepted Manuscripts* in the [Information for Authors](#).

Please note that technical editing may introduce minor changes to the text and/or graphics, which may alter content. The journal's standard [Terms & Conditions](#) and the [Ethical guidelines](#) still apply. In no event shall the Royal Society of Chemistry be held responsible for any errors or omissions in this *Accepted Manuscript* or any consequences arising from the use of any information it contains.

COMMUNICATION

Synthesis and Electrocatalytic Performance of Atomically Ordered Nickel Carbide (Ni₃C) Nanoparticles

Cite this: DOI: 10.1039/x0xx00000x

Received 00th January 2012,

Accepted 00th January 2012

DOI: 10.1039/x0xx00000x

www.rsc.org/

Nor A. Fadil,^{†,§} Govindachetty Saravanan,^{†,‡,§} Gubbala V. Ramesh^{*,†}, Futoshi Matsumoto,^{§§} Hideki Yoshikawa,[†] Shigenori Ueda,[†] Toyokazu Tanabe,[†] Toru Hara,[†] Shinsuke Ishihara,[†] Hideyuki Murakami,[†] Katsuhiko Ariga,^{†,‡} and Hideki Abe^{*,†,¶}

Atomically ordered nickel carbide, Ni₃C, was synthesized by reduction of nickel cyclopentadienyl (NiCp₂) with sodium naphthalide to form Ni clusters coordinated by Cp (Ni-Cp clusters). Ni-Cp clusters were thermally decomposed to Ni₃C nanoparticles smaller than 10 nm. The Ni₃C nanoparticles showed better performance than Ni nanoparticles and Au nanoparticles in electrooxidation of sodium borohydride.

Energy generation by polymer electrolyte membrane fuel cells (PEMFCs) has become increasingly critical as an alternative to combustion engines.¹⁻³ In particular, PEMFCs using more transportable and energetically dense fuels than hydrogen, direct-methanol fuel cells (DMFCs) and direct-borohydride fuel cells (DBFCs), are a focal point of interest.⁴⁻⁶ DBFCs have advantages over DMFCs in terms of output voltage because the oxidation potential of borohydrides is much lower than that of methanol or hydrogen.⁷⁻⁹ DBFCs require metal catalysts on anodes to complete the electrooxidation of borohydrides. Precious metals, including Pt, Pd and/or Au, are excellent catalysts, but they are expensive.¹⁰⁻¹³ Ni might be an alternative to precious metals because of its low cost and corrosion resistance in the alkaline electrolytes used in DBFCs, but it has poor catalytic activity. In particular, the high onset potential of Ni toward the electrooxidation of borohydrides, which is higher than those of the precious metals by +0.4 V or more, diminishes the applicability of Ni to DBFCs.¹⁴⁻¹⁵ We and our collaborators have recently demonstrated that ordered alloys of Pt and electronegative elements, such as PtPb and PtBi, are superior anode catalysts to pure Pt, especially in terms of the lower onset potentials for the electrooxidation of methanol.¹⁶⁻²¹ The discovery of PtPb and PtBi has prompted research for efficient anode catalysts in DBFCs among the ordered alloys of Ni and electronegative elements including carbon.

Here, we report that an atomically ordered nickel carbide, Ni₃C, can be synthesized in the form of nanoparticles (Nps) smaller than 10 nm and is expected to be an excellent anode catalyst for DBFCs. Nickel carbides have been previously synthesized as bulk materials, films or particles through mechanical alloying or the pyrolysis of organometallic compounds but have not been applied to catalysis, likely due to the large particle size (> 40 nm), resulting in low

surface areas.²²⁻²⁴ As illustrated in Figure 1, we first reduce nickel cyclopentadienyl (NiCp₂) with sodium naphthalide (NaNaph) in dry tetrahydrofuran (THF) at room temperature to obtain Cp-coordinated Ni clusters (Ni-Cp clusters).²⁵⁻²⁶ Ni-Cp clusters are then heated at 200 °C in vacuum to yield nanoparticles of Ni₃C with an average size of 6 nm. The Ni₃C Nps exhibit a better catalytic activity than synthesized Ni Nps toward the electrooxidation of NaBH₄ because of the low onset potential close to that of Au Nps.

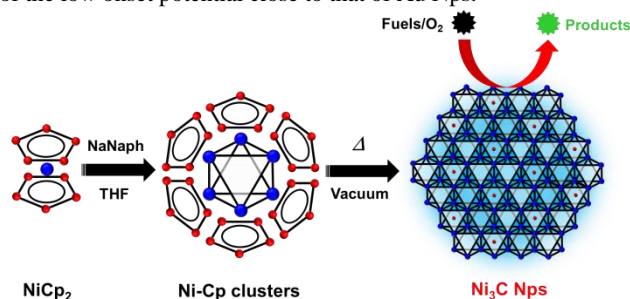


Figure 1. Synthetic scheme for Ni₃C Nps through chemical reduction of NiCp₂.

Ultrahigh-vacuum transmission electron microscopes (UHV-TEM) showed that the synthesized Ni₃C Nps were spherical and ranged in size from 3 to 9 nm (Figure 2a, 2b). Ordered lattice fringes were observed on the Ni₃C Nps, showing that the Nps were atomically ordered (Figure 2c). The interval of the lattice fringe, calculated as 0.201 nm from the Fourier-transformation image (inset of Figure 2c), was consistent with the *d*-value of the Ni₃C (113) plane (*d*₁₁₃ = 0.201 nm).^{22,23,27} The synthesized Ni₃C Nps were much smaller in size than the previously prepared Ni₃C materials, most likely because Ni-Cp clusters acted as an effective precursor, promoting the formation reaction at low temperatures.

Ni-Cp clusters were obtained by reduction of NiCp₂ with NaNaph as a black, air-sensitive powder.²⁵⁻²⁶ Fourier-transform infrared spectroscopy (FTIR) demonstrated that both the C=C- and in-plane C-H stretching modes of Cp molecules in the Ni-Cp clusters were dispersed in wavenumber and blue-shifted relative to those in NiCp₂ (Figure S1).²⁸ The powder X-ray diffraction (*p*XRD) profile for the

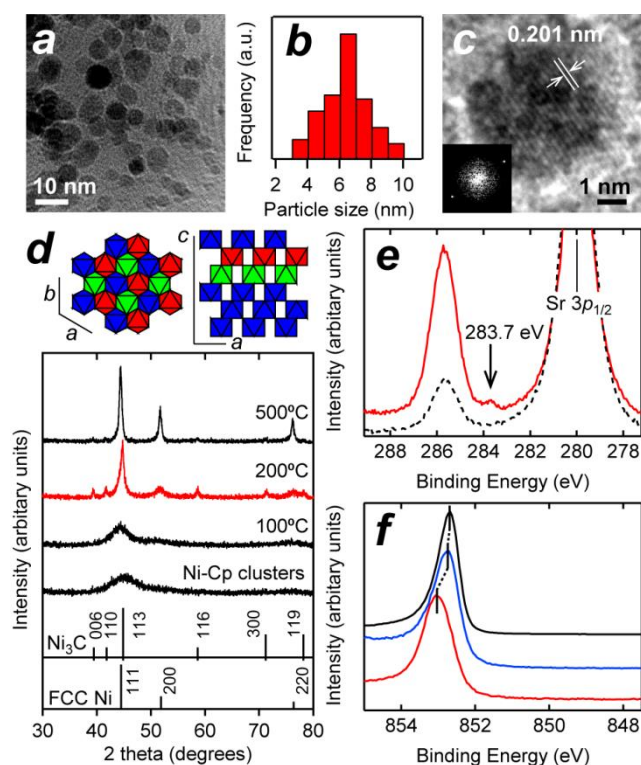


Figure 2. (a) Bright-field TEM image, (b) particle-size distribution and (c) high-resolution TEM image of Ni₃C Nps. Inset shows a Fourier-transformation image of this TEM image. (d) pXRD profiles for Ni-Cp clusters and the products obtained by annealing Ni-Cp clusters at different temperatures. Structural models for Ni₃C are presented at the top. The polyhedra correspond to Ni₆C-octahedra. Simulated pXRD peaks for Ni₃C and FCC-type Ni are shown by solid markers at the bottom. (e) HX-PES profiles in the C 1s region for Ni₃C Nps (red) and a SrTiO₃ substrate (black broken curve). (f) HX-PES profiles in the Ni 2p_{3/2} region for bulk Ni (black), Ni Nps (blue) and Ni₃C Nps (red). The inset shows HX-PES profiles in the valence region.

Ni-Cp clusters had a single peak at 45.0 degrees, which was slight larger than the reported 111 reflection angle for FCC-type Ni (*Fm*3 *m*, *a* = 0.352 nm), 44.5 degrees (Figure 2d).²⁹ The reflection peak shifted toward lower angles when the material was annealed in vacuum at 100 °C. Small reflection peaks became visible upon annealing at 200 °C at 39.3, 41.8, 58.7 and 71.4 degrees (red curve), corresponding to the 006, 110, 116 and 300 reflections of the Ni₃C Nps (*R*3c; *a* = 0.455 nm, *c* = 1.29 nm), respectively.^{22, 23, 27} A broad peak was recognized at 51.5 degrees corresponding to the 200 reflection of an impurity phase, FCC-type Ni. The Ni₃C Nps were decomposed to FCC-type Ni and carbon when the annealing temperature exceeded 500 °C, consistent with reports in the literature.³⁰⁻³¹

Hard X-ray photoemission measurements (HX-PES; photon energy = 5.95 keV) were performed on the Ni₃C Nps (Figures 2e, 2f and).³² The C1s photoemission peak was recognized on the Ni₃C Nps at 283.7±0.2 eV, in addition to the C 1s- (285.7±0.2 eV) and Sr 3p_{1/2} (280.0±0.2 eV) photoemission peaks from the substrates. The binding energy of Ni 2p_{3/2} photoemission peak for the Ni₃C Nps was 0.2 eV larger than those for bulk Ni and Ni Nps (Figure 2f). Both of the binding energies of the C 1s- and Ni 2p_{3/2} peaks for the Ni₃C Nps were consistent with those reported in the literature.^{23,34} The

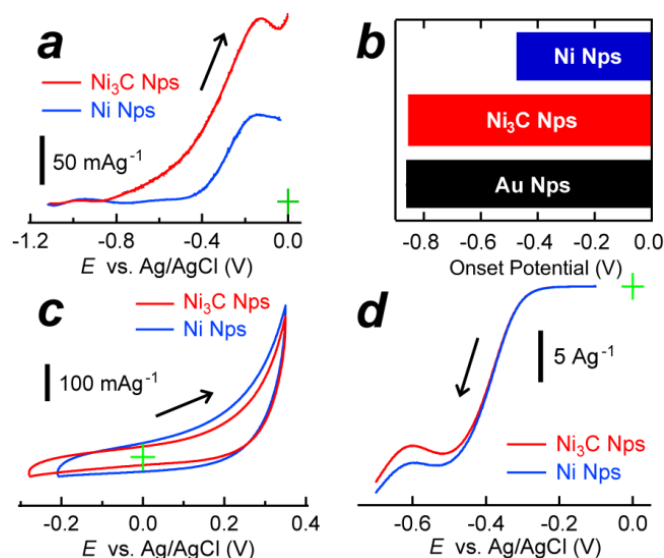


Figure 3. (a) Line-scan voltammograms for the electro-oxidation of NaBH₄ over the Ni₃C- and the Ni Nps. (b) Onset potentials of the Ni- (blue), Ni₃C- (red) and Au (black) Nps toward the electrooxidation of NaBH₄. (c) Cyclic voltammograms for the electrooxidation of methanol and (d) line-scan voltammograms for the oxygen reduction reaction (ORR) over the Ni₃C- and Ni Nps.

chemical composition of the Ni₃C Nps was calculated as Ni : C = 1.0 : 0.31±0.03 from a wide-range HX-PES data (S7), indicating that the desired, stoichiometric Ni₃C Nps were successfully materialized.

The electrocatalytic activity of the Ni₃C Nps was tested for different reactions in PEMFCs. Figure 3a shows line-scan voltammograms (LV) for the electrooxidation of NaBH₄ over the Ni₃C Nps and the Ni Nps (average size = 3 nm, see Figures S9-11). The mass activity of the Ni Nps started to increase at an onset potential of -0.43 V. The Ni₃C Nps showed an increase in the LV curve at an onset potential of -0.85 V, which was 0.42 V lower than the onset potential of the Ni Nps and close to that of Au Nps, -0.86 V (Figure 3b, see Figure S12 for details). In addition, the mass activity of the Ni₃C Nps was, at -0.4 V, 6.5 times larger than that of the Ni Nps. The Ni₃C Nps were more catalytically active than the Ni Nps toward the electrooxidation of NaBH₄, in terms of the lower onset potential and the larger mass activity.

Unlike the case of the electrooxidation of NaBH₄, the Ni₃C Nps were as catalytically active as the Ni Nps toward both the electrooxidation of methanol and the oxygen-reduction reaction (ORR). Figure 3c shows cyclic voltammograms (CV) for the electrooxidation of methanol over the Ni₃C- and Ni Nps in a range from -0.3 to +0.35 V. The CV curve for the Ni₃C Nps was similar to that for the Ni Nps over the entire potential range (Figure S11). Figure 3d shows LV curves for ORR over the Ni₃C- and Ni Nps. The Ni₃C- and Ni Nps had the same onset potential, -0.3 V, and their mass activities at the half-wave potential were virtually the same. Moreover, it was demonstrated that the Ni₃C Nps can retain their chemical composition and crystal structure even when subjected to repeated CV cycles in the NaBH₄ solution (S8, see the corresponding caption for details). Although Ni₃C is a thermally meta-stable phase³⁰⁻³¹, the synthesized Ni₃C Nps can work as a durable catalyst for the repeated operation of DBFCs.

The Ni₃C- and Ni Nps exhibited the same mass activities toward methanol electrooxidation and ORR, which indicates that the

enhanced NaBH_4 -electrooxidation activity of the Ni_3C Nps may be attributed to the inherent electronic property of the Ni_3C Nps, not to the size or dispersity of the Nps. As shown in Figure S6, the Ni_3C Nps had a depleted density-of-state (DOS) near the Fermi level (EF) due to strong hybridization between the Ni $3d$ - and C $2p$ orbitals. It is known that ever developed Ni-based alloys are good catalysts for the hydrolysis of BH_4^- but not for the electrooxidation of fuels because of the predominant adsorption of OH^- to the Ni surface.³⁵ The depleted DOS at the EF of the Ni_3C Nps can weaken the adsorption of OH^- to inhibit the formation of insulating $\text{Ni}(\text{OH})_2$ surface layers, resulting in the enhanced electrooxidation activity of BH_4^- over the Ni_3C Nps.

In conclusion, we have successfully synthesized the smallest Ni_3C Nps ever produced through thermal decomposition of Ni-Cp clusters. The Ni_3C Nps exhibited a catalytic activity superior to that of Ni Nps in the electrooxidation of NaBH_4 , demonstrating their applicability to DBFCs. The successful development of an electrode catalyst comprising Ni_3C Nps will promote the use of catalytic carbides in precious-metal-free PEFCs, which will help address the energy challenges that we face^{36,37}

This work was preliminarily supported by the JST PRESTO program, the Ministry of Education, Culture, Sports, Science and Technology (MEXT) and the Japan Society for the Promotion of Science (JSPS) through Grant-in-Aid 23560855. The HX-PES measurements were performed under the approval of the NIMS Beamline Station (Proposal No.2010B4609). The authors are grateful to HiSOR, Hiroshima University, and JAEA/Spring-8 for the development of HX-PES at BL15XU of Spring-8.

Notes and references

[†] National Institute for Materials Science (NIMS), 1-1 Namiki, Tsukuba, Ibaraki 305-0044, Japan

[§] Universiti Teknologi Malaysia, 81310 Skudai, Johor Bahru, Johor, Malaysia

[‡] CSIR-National Environmental Engineering Research Institute (CSIR-NEERI), Environmental Materials Division, Nehru Marg, Nagpur 440020, India.

^{§§} Kanagawa University, 3-27 Rokkakubashi, Yokohama, Kanagawa 221-8686, Japan

^{††} NIMS Beamline Station at Spring-8, National Institute for Materials Science (NIMS), 1-1-1 Kouto, Sayo, Hyogo 679-5148, Japan

^{†††} MANA, National Institute for Materials Science (NIMS), 1-1 Namiki, Tsukuba, Ibaraki 305-0044, Japan

^{††††} CREST, Japan Science and Technology Agency (JST), 1-1 Namiki, Tsukuba, Ibaraki 305-0044, Japan

^{†††††} PRESTO, Japan Science and Technology Agency (JST), 4-1-8 Honcho Kawaguchi, Saitama 332-0012, Japan

e-mail:

Abe.Hideki@nims.go.jp, GUBBALA.Venkataramesh@nims.go.jp

Electronic Supplementary Information (ESI) available: experimental details, compound syntheses and characterization, and additional data. See DOI: 10.1039/c000000x/

1 H. A. Gasteiger and N. M. Marković, *Science*, 2009, **324**, 48.

2 R. Borup, J. Meyers, B. Pivovar, Y. S. Kim, R. Mukundan, N. Garland, D. Myers, M. Wilson, F. Garzon, D. Wood, P. Zelenay, K. More, K. Stroh, T. Zawodzinski, J. Boncella, J. E. McGrath, M. Inaba, K. Miyatake, M. Hori, K. Ota, Z. Ogumi, S. Miyata, A. Nishikata, Z. Siroma, Y. Uchimoto, K. Yasuda, K. I. Kimijima and N. Iwashita, *Chem. Rev.* 2007, **107**, 3904.

3 H. A. Gasteiger, S. S. Kocha, B. Sompalli and F. T. Wagner, *Appl. Catal. B* 2005, **56**, 9.

4 E. Reddington, A. Sapienza, B. Gurau, R. Viswanathan, S. Sarangapani, E. S. Somtkin and T. E. Mallouk, *Science* 1998, **280**, 1735.

5 Liu, B. H.; Li, Z. P. *J. Power Sources*, 2009, **187**, 527.

6 J. H. Wee, *J. Power Sources* 2006, **155**, 329.

7 K. Wang, J. Lu and L. Zuang, *Catal. Today* 2011, **170**, 99.

8 Z. P. Li, B. H. Liu, K. Arai and S. Suda, *J. Alloy. Compd.* 2005, **404**, 648.

9 B. H. Liu, Z. P. Li, K. Arai and S. Suda, *Electrochim. Acta* 2005, **50**, 3719.

10 P. He, Y. Wang, F. Pei, H. Wang, L. Liu and L. Yi, *J. Power Sources* 2011, **196**, 1042.

11 G. Guella, B. Patton and A. Miotello, *J. Phys. Chem. C* 2007, **111**, 18744.

12 M. Chatenet, F. Micoud, I. Roche and E. Chainet, *Electrochim. Acta* 2006, **51**, 5459.

13 J. H. Kim, H. S. Kim, Y. M. Kang, M. S. Song, S. Rajendran, S. C. Han, D. H. Jung, J. Y. Lee, *J. Electrochem. Soc.* 2004, **151**, A1039.

14 H. Çelikkan, M. Şahin, M. L. Aksu and T. N. Veziroğlu, *Int. J. Hydrogen Energy* 2007, **32**, 588.

15 B. H. Liu, Z. P. Li and S. Suda, *J. Electrochem. Soc.* 2003, **150**, A398.

16 Y. Liu, M. A. Lowe, F. J. DiSalvo and H. D. Abruña, *J. Am. Chem. Soc.* 2010, **114**, 14929.

17 Y. Liu, H. Abe, H. M. Edverson, F. J. DiSalvo and H. D. Abruña, *Phys. Chem. Chem. Phys.* 2010, **12**, 12978.

18 L. R. Alden, C. Roychowdhury, F. Matsumoto, D. K. Han, V. B. Zeldovich, H. D. Abruña and F. J. DiSalvo, *Langmuir* 2006, **22**, 10465.

19 C. Roychowdhury, F. Matsumoto, V. B. Zeldovich, S. C. Warren, P. F. Mutolo, M. Ballesteros, U. Wiesner, H. D. Abruña and F. J. DiSalvo, *Chem. Mater.* 2006, **18**, 3365.

20 L. R. Alden, D. K. Han, F. Matsumoto, H. D. Abruña and F. J. DiSalvo, *Chem. Mater.* 2006, **18**, 5591.

21 E. Casado-Rivera, D. J. Volpe, L. R. Alden, C. Lind, C. Downie, T. Vázquez-Alvarez, A. C. D. Angelo, F. J. DiSalvo and H. D. Abruña, *J. Am. Chem. Soc.* 2004, **126**, 4043.

22 Z. L. Schaefer, K. M. Weeber, R. Misra, P. Schiffer and R. E. Schaak, *Chem. Mat.* 2011, **23**, 2475.

23 Y. Goto, K. Taniguchi, T. Omata, S. Otsuka-Yao-Matsuo, N. Ohashi, S. Ueda, H. Yoshikawa, Y. Yamashita, H. Ohashi and K. Kobayashi, *Chem. Mater.* 2008, **20**, 4156.

24 Y. G. Leng, Y. Liu, X. B. Song and X. G. Li, *J. Nanosci. Nanotechnol.* 2008, **8**, 4477.

25 M. S. Paquette and L. F. Dahl, *J. Am. Chem. Soc.* 1980, **102**, 6621.

26 H. W. Chiu and S. M. Kauzlarich, *Chem. Mat.* 2006, **18**, 1023.

27 L. He, *J. Magn. Magn. Mater.* 2010, **322**, 1991.

28 É. Bencze, B. V. Lokshin, J. Mink, W. A. Herrmann and F. E. Kühn, *J. Organomet. Chem.* 2001, **627**, 55.

29 *Pearson's Handbook of Crystallographic Data for Intermetallic Phases*; P. L. Villars, L. D. Calvert, Eds.; American Society of Metals: Metals Park, OH, USA, 1985.

30 S. Nagakura, *J. Phys. Soc. Jpn.* 1958, **13**, 1005.

31 S. Nagakura, *J. Phys. Soc. Jpn.* 1957, **12**, 482.

32 T. Ohsawa, Y. Adachi, I. Sakaguchi, K. Matsumoto, H. Haneda, S. Ueda, H. Yoshikawa, K. Kobayashi and N. Ohashi, *Chem. Mat.* 2009, **21**, 144.

33 G. J. Kovács, I. Bertóti and G. Radnóczy, *Thin Solid Films* 2008, **516**, 7942.

34 L. Yue, R. Sabiryanov, E. M. Kirkpatrick and D. L. Leslie-Pelecky, *Phys. Rev. B* 2000, **62**, 8969.

35 F. Gopal, Y. Valadbeigi and L.M. Kasmae, *J Electroanal Chemistry*, 2011, **650**, 219.

36 C. D. A. Brady, E. J. Rees and G. T. Burstein, *J. Power Sources* 2008, **179**, 17.

37 M. Nagai, M. Yoshida and H. Tominaga, *Electrochim. Acta*, 2007, **52**, 5430.